Pressure Optimization for Hydraulic-Electric Hybrid Biped Robot Power Unit Based on Genetic Algorithm

Pengyu Zhao (zhaopengyu@zhejianglab.com)
Zhejiang Lab https://orcid.org/0000-0002-0514-2548
Anhuan Xie
Zhejiang Lab
Shiqiang Zhu
Zhejiang Lab
Lingyu Kong
Zhejiang Lab
Dan Zhang
Zhejiang Lab

Research Article

Keywords: biped robot, hybrid drive, hydraulic power unit, pressure optimization, genetic algorithm

Posted Date: June 23rd, 2022

DOI: https://doi.org/10.21203/rs.3.rs-1598888/v1

Pressure Optimization for Hydraulic-Electric Hybrid Biped Robot Power Unit Based on Genetic Algorithm

Pengyu Zhao[1*], Anhuan Xie[1,2], Shiqiang Zhu[1,2], Lingyu Kong[1], Dan Zhang[1,3]

1. *Zhejiang Lab, 1818 West Wenyi Road, Hangzhou , Zhejiang 311121, P. R. China*
2. *Zhejiang University, 38 Zheda Road, Hangzhou, Zhejiang 310027, P.R. China*
3. *York University, Toronto, Canada*

Corresponding author: Pengyu Zhao E-mail: zhaopengyu@zhejianglab.com

Abstract: Biped robot has attracted increasing attention because of its flexible movement and strong adaptability to the surroundings. However, the small output torque and the weak impact resistance of motor drive, as well as the large energy consumption of hydraulic drive limit the performance of biped robot drive system. Aiming at these shortcomings, an electric-hydraulic hybrid drive system of biped robot was proposed in this paper. The robot platform was designed based on the prototype of Zhejiang Lab biped robot. The mathematical model of hydraulic drive system and the simulation model of mechanical structure were established to analyze the dynamic characteristic and the load force during walking. The value function reflecting the energy consumption of the hydraulic drive system was proposed. The pressure of the accumulator in the hydraulic power unit was selected as the control parameter. In order to get the minimum value of the value function, so as to reduce the energy consumption of the hydraulic driving system, the control parameters were optimized by genetic algorithm. From the simulation results, the proposed optimization algorithm can improve the efficiency by 3.49%.

Key Words: biped robot, hybrid drive, hydraulic power unit, pressure optimization, genetic algorithm

1 Introduction

Mobil robots can be categorized as wheeled, tracked and legged type according to the different modes of movement. Among them, legged robots have been paid increasing attention because of their flexible movement and strong adaptability to the surroundings. The driving modes of legged robots developed in recent years mainly include motor drive and hydraulic drive[1].

Hydraulic drive has many excellent characteristics, making it an ideal choice for high dynamic articulated robots. On one hand, the power density of hydraulic drive is high[2]. For example, the power density of Shandong University SCALF-III robot[3] which is driven by hydraulic system, can reach 7kW/kg, while the power density of EC60-400W robot[4] and TBM(S)-12913-B robot[5] which are driven by motor, is 0.17kW/kg and 0.43kW/kg, respectively. On the other hand, gear transmission is not necessary in a hydraulic drive system, which makes it possible to absorb large impact load[6]. Hence, the impact resistance robustness, stiffness and bandwidth are improved. However, the low energy efficiency and serious heating of hydraulic system have become one of the important factors limiting its development[7].

The hydraulic drive system can be divided into closed pump control system and open valve control system according to the different control components.

The closed pump control system does not need a large hydraulic tank. Thus, the weight and volume of the hydraulic power unit is reduced. Also, throttling loss is avoided, which can significantly improve the efficiency of the hydraulic system and shows obvious advantages in energy saving[8]. In a typical closed system, the oil inlet and outlet of the actuator are connected to the two oil outlets of the hydraulic pump respectively. The speed and movement direction of the actuator are controlled by adjusting the rotational speed or displacement of the hydraulic pump. For example, the direct

pump-controlled system utilized in legged robots can avoid the throttling loss of the servo valves and achieve high energy efficiency[9][10]. However, since the inertia mass (or moment of inertia) of a hydraulic pump variable mechanism or the rotor of a motor is much larger than that of a valve core, the response speed of the pump control system is usually slow. The load adaptability and controllability are not as good as a valve control system. Usually, the closed pump control system has a good driving effect for the system with slow motion or low requirement of response speed and control precision. It is still difficult to be applied to legged robot.

The open valve control system, especially the servo valve controlled hydraulic actuator, has become the main driving mode of the robot hydraulic drive system. The servo valve has a high response characteristic, which meets the requirements of a robot drive system. Also, the control algorithm is mature with good control effect. For example, the biped robots like BBH from Bath University[11], NWPUBR-1 from Northwestern Polytechnical University[12], and the quadruped robots like Hydraulically-powered Quadruped (HyQ) robots from the Institute of Technology in Italy[13][14][15], SCalf from Shandong University[16][17] and quadruped robot from Yanshan University[18][19][20] are all driven by servo valve controlled cylinders. However, in an open valve control system with centralized power source, the power unit should always maintain a high pressure to ensure that the system has a high response characteristic. When the output force of the actuator is small, the power unit still needs to supply oil at the highest pressure, which leads to a large throttling loss of the valve port. Then the energy efficiency of the system is reduced and the heat generated by the valve is increased.

In order to reduce the energy consumption of the hydraulic drive system, the difference between the demand pressure of the actuator and the supplied pressure of the power unit should be reduced to minimize the pressure drop of the control valve. For example, multi pump hydraulic power unit with valve matrix is one of the attempts[21]. This power unit can significantly increase the energy utilization rate. But it increases the weight of the hydraulic system. So, the improvement of the total energy efficiency of the robot is limited

According to the analysis above, based on the biped robot platform proposed by Zhejiang Lab, an electric-hydraulic hybrid drive system is proposed in this paper. The drive system makes full use of the advantages of high efficiency of motor drive and large power density of hydraulic drive. Aiming at the shortage of large energy loss and low efficiency of the hydraulic system, the pressure of the power unit is optimized and the control strategy is put forward.

2 System Configuration

2.1 Mechanical Construction

The prototype of the Zhejiang Lab biped robot consists of a trunk, hips, thighs, calves and feet, which are hinged between adjacent body structures. There is a degree of freedom (DOF) of turnover to control the abduction/adduction of the leg and a freedom of yaw to control the direction of the leg between the hip and the thigh. The two DOFs provide no vertical bearing capacity, which reduces the demand torque. So, they are designed to be driven by electric motors.

The hip joint, knee joint and ankle joint each have a DOF of rotation. The driving torque of the hip joint and knee joint is large. The peak value of the driving torque of the two joints exceeds the maximum output torque of the electric motor under the impact load. So, the hydraulic drive is utilized. In the underdrive gait algorithm based on virtual constraint, the ankle joint only controls the foot to be parallel to the ground, and the required torque is small. So, it is also driven by an electric motor.

In order to reduce the moment of inertia of moving parts, actuators should be centrally installed on non-moving parts such as hip, or on the structures with small rotation radius such as upper thigh. For this purpose, the hip turnover and yaw motors are fixedly attached to the trunk and hips

respectively. They are mounted coaxially with the rotating shaft. The ankle is driven by an electric motor mounted on the hip through two sets of connecting rods. The hip hydraulic cylinder is hinged to the hip and thigh. The knee hydraulic cylinder is hinged to the thigh and calf. The structure of the designed hybrid drive robot is shown in Fig.1.

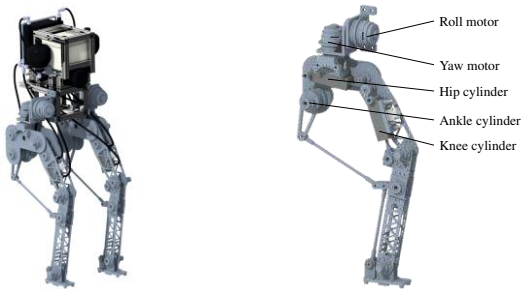

Figure 1 Mechanical structure of hybrid drive robot

The geometric dimension of each structure is shown in Table 1.

Table 1 Geometric dimension of each structure

Structure	Length/mm
Hip	200
Thigh	300
Calf	430
Foot	120

2.2 Hydraulic System

In order to improve the response of the system and realize accurate position control, the servo valve controlled hydraulic cylinders are utilized as the actuators. The rated pressure of the hydraulic system is 21MPa. Based on the calculation, the pressure of the hydraulic cylinder is generally no more than 10MPa under normal walking conditions, and the pressure is high only under the impact load or the instantaneous rapid movement. If the outlet pressure of the pump is maintained at the rated pressure all the time, the pressure difference between the pressure port and the working ports of the servo valve is large, which increases the throttling loss of the servo valve and the input power of the hydraulic pump, resulting in a very low system efficiency. From simulation analysis, if the oil maintains 21MPa constant pressure, the efficiency of the hydraulic system is only about 10% in the walking condition.

In order to improve the efficiency of the system, the accumulators in high and low working pressures are used to supply oil to the system. The hydraulic pump charges the accumulator respectively according to the charging state of each accumulator. Each hydraulic cylinder access to the high-pressure or low-pressure circuit according to the demand pressure, controlled by a directional valve. The principle of the hydraulic system is shown in Fig.2.

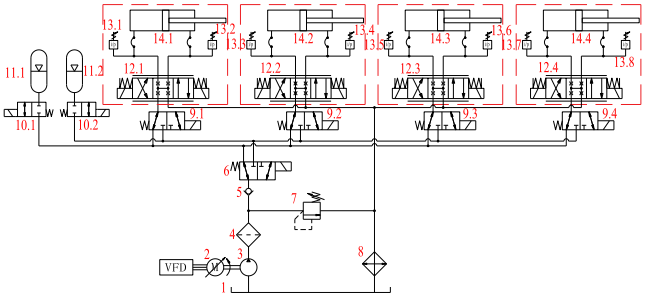

1 Oil tank, 2 Variable frequency motor, 3 Hydraulic pump, 4 Filter, 5 Check valve, 6 Two-position three-way directional control valve, 7 Relief valve, 8 Cooler, 9 Two-position three-way directional control valve, 10 Switch valve, 11 Accumulator, 12 Servo valve, 13 Pressure sensor, 14 Hydraulic cylinder.

Figure 2 Principle of hydraulic system

In the system, 11.1 is a low-pressure accumulator and 11.2 is a high-pressure accumulator. The following is an example to introduce the working principle. When the pressure in the hydraulic cylinder 14.1 is lower than the set pressure of the low-pressure accumulator, the directional valve 9.1 connects the cylinder 14.1 to the low-pressure accumulator circuit. At this time, the pressure at the oil inlet P of the servo valve 12.1 is low. When the cylinder 14.1 drives the joint, the oil in the low-pressure accumulator is consumed. On the contrary, when the pressure in the cylinder 14.1 is higher than the set pressure of the low-pressure accumulator, the directional valve 9.1 connects the cylinder 14.1 to the high-pressure accumulator circuit. At this time, the pressure at the oil inlet P of the servo valve 12.1 is high pressure, and the oil in the high-pressure accumulator is consumed when the hydraulic cylinder 14.1 acts. The hydraulic pump 3 charges liquid to the low-pressure accumulator or high-pressure accumulator through the directional valve 6. In this system, the hydraulic pump charges the low-pressure accumulator most of the time, and the outlet pressure of the pump is only the low-pressure

accumulator pressure. So, the energy consumption of the hydraulic pump can be reduced

According to the load of the robot, the parameters of the main components are calculated, as shown in Table 2.

Table 2 Main components parameters of hydraulic system

Components	Parameter	Value
Pump	Rated pressure/MPa	21.0
	Displacement/mL·r^{-1}	4.0
	Range of speed/rpm	0~4000
Cylinder	Diameter of piston rod/mm	10
	Diameter of piston/mm	25
	Stroke/mm	50
Servo valve	Rated flow rate/ L·min^{-1} (@7MPa pressure drop)	6.9
	Response frequency/Hz	200
	Damping ratio	0.5
Accumulator	Volume/L	2.6
	Rated pressure/MPa	21.0

3 Mathematical Model

In order to simplify the mathematical model of the hydraulic system, the following assumptions are made:

(1) The flow coefficient of each throttle port of the servo valve is equal, that is: C_{d1}= C_{d2}= C_{d3}= C_{d4}= C_d;

(2) The throttle port of the servo valve is rectangular, with area gradient W and displacement of the valve core x_v. Then the throttle port area is $W \cdot x_v$;

(3) The pressure in the same chamber of the hydraulic cylinder is equal everywhere. The oil temperature and the volume elastic modulus are constant;

(4) The internal leakage and external leakage of the hydraulic cylinder is laminar flow.

3.1 Servo Valve

For an ideal zero-opening slide valve, all four control throttles are closed when the spool is in the middle of the sleeve.

When PA port of the servo valve is conducting, $x_v > 0$,

$$q_{vA}=C_d W x_v \sqrt{\frac{2}{\rho}\left(p_{vP}-p_{vA}\right)} \tag{1}$$

$$q_{vB}=C_d W x_v \sqrt{\frac{2p_{vB}}{\rho}} \tag{2}$$

When PB port of the servo valve is conducting, $x_v < 0$,

$$q_{vA}=C_d W x_v \sqrt{\frac{2p_{vA}}{\rho}} \tag{3}$$

$$q_{vB}=C_d W x_v \sqrt{\frac{2}{\rho}\left(p_{vP}-p_{vB}\right)} \tag{4}$$

Where, q_{vA} is the flow rate of the servo valve port A; q_{vB} is the flow rate of port B; p_{vP} is the pressure of port P; p_{vA}, p_{vB} is the pressure of port A and port B respectively; ρ is the density of liquid.

The load pressure of the ideal zero-opening four-slide valve is defined as:

$$p_{vL} = p_{vA} - k_c p_{vB} \tag{5}$$

Where, k_c is the area ratio of the hydraulic cylinder piston side and rod side. The pressure-flow characteristic equation can be expressed as:

$$q_{vL}=C_d W x_v \sqrt{\frac{1}{\rho}\left(p_{vP}-\frac{x_v}{|x_v|}p_{vL}\right)} \tag{6}$$

The flow gain of the slide valve is:

$$K_q=\frac{\partial q_{vL}}{\partial x_v}=C_d W\sqrt{\frac{1}{\rho}\left(p_{vP}-p_{vL}\right)} \tag{7}$$

The pressure-flow coefficient is:

$$K_c=-\frac{\partial q_{vL}}{\partial p_{vL}}=\frac{C_d W x_v\sqrt{\frac{1}{\rho}\left(p_{vP}-p_{vL}\right)}}{2\left(p_{vP}-p_{vL}\right)} \tag{8}$$

The pressure gain is:

$$K_p=\frac{\partial p_{vL}}{\partial x_v}=\frac{2\left(p_{vP}-p_{vL}\right)}{x_v} \tag{9}$$

The servo valve internal leakage is simplified as:

$$q_{vil}=K_{vil}q_{vL}+C_{vil} \tag{10}$$

Where, K_{vil} is a proportionality coefficient; C_{vil} is a constant.

3.2 Hydraulic Cylinder

Firstly, the flow continuity equation is established. The flow into the piston side of the hydraulic cylinder is:

$$q_{cA} = A_{cA}\frac{dx_p}{dt} + C_{ci}\left(p_{cA} - p_{cB}\right) + C_{ce}p_{cA} + \frac{V_{cA}}{\beta_e}\frac{dp_{cA}}{dt} \quad (11)$$

The flow out of the rod side is:

$$q_{cB} = A_{cB}\frac{dx_p}{dt} + C_{ci}\left(p_{cA} - p_{cB}\right) - C_{ce}p_{cB} - \frac{V_{cB}}{\beta_e}\frac{dp_{cB}}{dt} \quad (12)$$

Where, q_{cA} is the flow into the piston side; q_{cB} is the flow out of the rod side; p_{cA}, p_{cB} are the pressure of piston side and rod side, respectively; A_{cA}, A_{cB} are the area of piston side and rod side respectively; x_p is the displacement of piston; C_{ci} and C_{ce} are the internal and external leakage coefficients of the hydraulic cylinder, respectively; β_e is the effective bulk elastic modulus of oil.

Secondly, the balance equation of the hydraulic cylinder is established. The balance equation of the output force and load force of the hydraulic cylinder is:

$$A_{cA}p_{cA} - A_{cB}p_{cB} = m_t\frac{d^2x_p}{dt^2} + B_p\frac{dx_p}{dt} + Kx_p + F_L \quad (13)$$

Where, m_t is the total mass of the piston and the load converted to the piston; B_p is the viscous damping coefficient of piston and load; K is the load spring stiffness; F_L is the external load acting on the piston rod.

3.3 Accumulator

According to Boyle's law, the thermodynamic equation of accumulator is:

$$p_a V_{a\_gas}^n = \text{const.} \quad (14)$$

Where, p_a is the pressure of the accumulator; V_{a_gas} is the gas volume in the accumulator; n is the polytropic exponent, which is determined by the working condition of the accumulator. In the proposed system, $n = 1.4$.

The volume of oil in the accumulator is:

$$V_{a\_oil} = V_a - V_{a\_gas} \quad (19)$$

Where V_a is the volume of the accumulator. Then, the energy stored in the accumulator can be calculated as:

$$E_a = 10^3 \cdot \int p_a dV_{a\_oil} \quad (20)$$

3.4 Pump

The input power of the hydraulic pump is:

$$P_p = T_p\omega_p \quad (21)$$

Where, T_p is the input torque; ω_p is the rotate speed.

The torque balance equation of the hydraulic pump can be expressed as:

$$T_p = J_p\frac{d\omega_p}{dt} + \beta_p\omega_p + \Delta p_p D_p \quad (22)$$

Where, J_p is the equivalent moment of inertia of the hydraulic pump; β_p is the viscous damping coefficient; Δp_p is the pressure difference between the outlet and the inlet; D_p is the displacement.

The flow rate of the hydraulic pump is:

$$q_{vp} = \eta_{vp}D_p\omega_p \quad (23)$$

Where, η_{vp} is the volumetric efficiency of the hydraulic pump.

The oil continuity equation of the hydraulic pump can be expressed as:

$$\frac{V_p}{\beta_e}\frac{dp_p}{dt} = q_{vp} - \frac{\omega_p D_p}{2\pi} - C_p\Delta p_p \quad (24)$$

Where, V_p is the volume of the pump outlet; p_p is the pressure of the pump outlet; C_p is the sum of the internal and external leakage coefficients of the hydraulic pump.

3.5 Load Force

The objective of this paper is to analyze the performance of the hydraulic drive system. In the proposed robot, only the hip joint and knee joint are driven by hydraulic system. The two DOFs of turnover and yaw of the leg, which controls the lateral movement, has little relation with the performance of the hydraulic system. In other words, the hydraulic system only drives the robot to move forward and backward, but not sideways. In order to simplify the simulation model, the robot movement is limited to a two-dimensional plane, which has no obvious effect on the analysis results of the hydraulic system.

The physical model of the mechanical structure of the leg is established. The robot is controlled to complete the

specified movements to obtain the load force and movement of each joint. The established model is shown in **Error! Reference source not found.**.

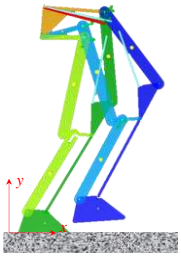

Figure 3 Robot mechanical structure model

The projection of the robot's gravity center on the ground at t=0 is taken as the coordinate origin; the forward direction of the robot parallel to the ground is taken as the positive direction of the x-axis; and the upward direction of the vertical ground is taken as the positive direction of the y-axis. The global coordinate system of the robot's motion is established.

In this paper, a specific movement is selected as an example. The energy consumption of the hydraulic drive system during the movement is calculated and analyzed.

The gait algorithm based on virtual constraint is used to control the robot to complete the movement of step - walk - step within 20s. During the movement, the gravity center position of the robot is shown in Fig.4, which also shows the projection of the gravity center on the x-t plane and the y-t plane.

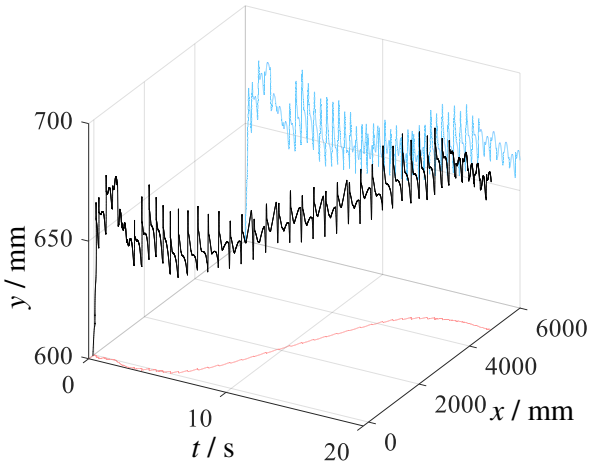

Figure 4 Gravity center position of robot

Based on the model above, parameters such as position, joint angle and actuator output force of the robot can be obtained.

3.6 Energy Consumption

According to the load force, the output power of the actuator can be calculated:

$$P_{\mathrm{c\_out}i} = F_{ci}\frac{\mathrm{d}x_{\mathrm{p}i}}{\mathrm{d}t} \tag{25}$$

Then, the active work done by the actuator is:

$$W_{\mathrm{c\_out}i} = \int_{t=0}^{t_{\mathrm{f}}} P_{\mathrm{c\_out}i}\cdot\mathrm{d}t \tag{26}$$

Where, x_{p} is the displacement of the piston; i=1,2,3,4 representing left hip, right hip, left knee and right knee, respectively; t_{f} is the end moment of movement. For the specific movement calculated in this paper, t_{f}=20s .

The overall power and active work of the hydraulic system can be respectively expressed as the sum of the output power and the sum of the active work of the four hydraulic actuators:

$$P_{\mathrm{out}} = \sum_{i=1}^{4} P_{\mathrm{c\_out}i} \tag{27}$$

$$W_{\mathrm{out}} = \sum_{i=1}^{4} W_{\mathrm{c\_out}i} \tag{28}$$

The input power of a single joint actuator can be expressed as:

$$P_{\mathrm{c\_in}i} = p_{\mathrm{vP}i}q_{\mathrm{vP}i} \tag{29}$$

Where, q_{vP} is the flow rate of servo valve port P.

The input power of the hydraulic system can be expressed as:

$$P_{\mathrm{in}} = P_{\mathrm{p}} \tag{30}$$

The energy consumed by the hydraulic system is:

$$W_{\mathrm{in}} = \int_{0}^{t_{\mathrm{f}}} P_{\mathrm{in}}\mathrm{d}t + \frac{\sum E_{\mathrm{a\_i}} - \sum E_{\mathrm{a\_f}}}{\eta_{\mathrm{a}}} \tag{31}$$

Where, $E_{\mathrm{a\_i}}$ is the energy stored in the accumulator at the beginning of the movement; $E_{\mathrm{a\_f}}$ is the energy stored in the accumulator at the end of the movement; η_{a} is the average efficiency when the hydraulic system charges the accumulator. We take η_{a}=95% .

4 Power Unit Pressure Optimization Algorithm

The purpose of the proposed power unit pressure optimization algorithm is to reduce the total input power and maintain adjusting the pressure of the accumulators. The algorithm also controls the hydraulic pump to charge the accumulators respectively at a certain flow rate.

The energy consumed by the hydraulic system is represented by the value function. In order to avoid the minimum value of the value function converging to the state where the difference between the highest pressure and the lowest pressure of the low-pressure accumulator is 0, the switching time interval of the reversing valve is introduced as the penalty function term:

$$J_{\mathrm{v}}=\int_{t=0}^{t_{\mathrm{f}}}\left(P_{\mathrm{in}}+k_{\mathrm{p}}\cdot\Delta t_{\mathrm{s}}\right)\mathrm{d}t \tag{32}$$

Where, Δt_{s} is the switching time interval; k_{p} is the coefficient of the penalty function term:

$$k_{\mathrm{p}}=\begin{cases}k_{\mathrm{ep}}\left(\dfrac{\Delta t_{\mathrm{set}}}{\Delta t_{\mathrm{s}}}+\dfrac{\Delta t_{\mathrm{s}}}{\Delta t_{\mathrm{set}}}-2\right) & \Delta t_{\mathrm{s}}<\Delta t_{\mathrm{set}}\\ 0 & \Delta t_{\mathrm{s}}\geq\Delta t_{\mathrm{set}}\end{cases} \tag{33}$$

Where, Δt_{set} is the ideal switching time interval of the reversing valve; k_{ep} is the coefficient.

The pressure of the high-pressure accumulator is determined by the rated pressure of the system and the demand pressure of the actuator. There is no need to optimize the pressure of high-pressure accumulator. Therefore, the pressure range of the high-pressure accumulator is set as 19~21MPa. That is, the minimum working pressure of the high-pressure accumulator is $p_{\mathrm{ah\_l}}$=19MPa and the maximum working pressure is $p_{\mathrm{ah\_h}}$=21MPa .

We assume that the lowest working pressure and the highest working pressure of the low-pressure accumulator are $p_{\mathrm{al\_l}}$ and $p_{\mathrm{al\_h}}$, respectively. In order to reduce the maximum input power of the hydraulic system, the hydraulic pump should charge the accumulators with approximately constant flow to avoid the instantaneous large flow of oil output. It is also assumed that the actuators consume the oil in the high/low pressure accumulator at a constant rate of $q_{\mathrm{ah\_out}}$ and $q_{\mathrm{al\_out}}$, respectively. The hydraulic pump charges the high/low pressure accumulator at the flow rate of $q_{\mathrm{ah\_in}}$ and $q_{\mathrm{al\_in}}$. It can be obtained by equaling the consuming time to the charging time:

$$\frac{\sqrt[n]{\dfrac{p_{\mathrm{ah\_h}}}{p_{\mathrm{ah\_l}}}}-1}{q_{\mathrm{ah\_out}}}=\frac{\sqrt[n]{\dfrac{p_{\mathrm{al\_h}}}{p_{\mathrm{al\_l}}}}-1}{q_{\mathrm{al\_in}}-q_{\mathrm{al\_out}}} \tag{34}$$

$$\frac{\sqrt[n]{\dfrac{p_{\mathrm{ah\_h}}}{p_{\mathrm{ah\_l}}}}-1}{q_{\mathrm{ah\_in}}-q_{\mathrm{ah\_out}}}=\frac{\sqrt[n]{\dfrac{p_{\mathrm{al\_h}}}{p_{\mathrm{al\_l}}}}-1}{q_{\mathrm{al\_out}}} \tag{35}$$

From the equations above, we can get $q_{\mathrm{ah\_in}}$ and $q_{\mathrm{al\_in}}$. Then the output flow rate of the pump is:

$$q_{\mathrm{p}}=k_{\mathrm{s}}q_{\mathrm{ah\_in}}+\left(1-k_{\mathrm{s}}\right)q_{\mathrm{al\_in}} \tag{36}$$

Where, k_{s} is the input signal of reversing valve. When the pump charges the high-pressure accumulator, k_{s}=1 . Otherwise, k_{s}=0 .

The power unit control rule is:

(1) In the initial state, the pressure in the high-pressure accumulator is the highest set working pressure $p_{\mathrm{ah\_h}}$, and the pressure in the low-pressure accumulator is the lowest set working pressure $p_{\mathrm{al\_l}}$.

(2) When the pressure in the low-pressure accumulator drops to the lowest set pressure $p_{\mathrm{al\_l}}$, the hydraulic pump charges the low-pressure accumulator with flow rate $q_{\mathrm{al\_in}}$ until the pressure reaches the highest set pressure $p_{\mathrm{al\_h}}$ and maintain the pressure.

(3) When the pressure in the high-pressure accumulator drops to the lowest set pressure $p_{\mathrm{ah\_l}}$, the hydraulic pump charges the high-pressure accumulator.

(4) When the pressure in the high-pressure accumulator reaches the highest set pressure $p_{\mathrm{ah\_h}}$, the hydraulic pump is

switched back to charge the low-pressure accumulator with flow rate $q_{\text{al\_in}}$.

The switching rule of the actuator access to the high/low pressure circuit is:

(1) When the pressure of the two chambers of the hydraulic cylinder is lower than the minimum set pressure of the low-pressure accumulator $p_{\text{al\_l}}$, the hydraulic cylinder is connected to the low-pressure circuit.

(2) When the pressure of either chamber of the hydraulic cylinder is higher than the minimum set pressure of the low-pressure accumulator $p_{\text{al\_l}}$, the hydraulic cylinder is connected to the high-pressure circuit.

The boundary conditions are:

$$p_{\text{al\_l}} \le p_{\text{al}} \le p_{\text{al\_h}} \tag{37}$$

$$p_{\text{ah\_l}} \le p_{\text{ah}} \le p_{\text{ah\_h}} \tag{38}$$

$$q_{\text{p\_min}} \le q_{\text{p}} \le q_{\text{p\_max}} \tag{39}$$

Where, $q_{\text{p\_min}}$ and $q_{\text{p\_max}}$ are the minimum and maximum output flow rate of the hydraulic pump.

The pressure range of the low-pressure accumulator is determined by genetic algorithm. The parameters of genetic algorithm are shown in Table 4.

Table 3 Parameter of genetic algorithm

Parameter	Value
Population quantity	50
Scaling function	Rank
Selection function	Stochastic uniform
Elite count	5
Crossover probability	0.8
Crossover function	Scattered
Mutation probability	0.2
Mutation interval	20

5 Simulation Verification

In order to verify the effectiveness of the proposed power unit pressure optimization algorithm, the hydraulic system parameters calculated by the optimization algorithm are used to simulate and analyze the robot movement described in Section 3. The energy consumption is compared with that without the optimization algorithm.

5.1 Pressure with Optimization

To reduce the error caused by short simulation time, the sum of the value function of 5 successive step – walk – step actions is taken as the value function of the genetic algorithm in the calculation. The optimal vale and average valve of the value function calculated by the genetic algorithm are shown in Fig.5.

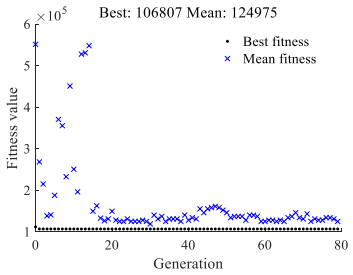

Figure 5 Genetic algorithm value function

The working pressure range of the accumulators calculated by the algorithm is shown in Table 5.

Table 4 Working pressure range of accumulator

Accumulator	Parameter	Value/MPa
High-pressure accumulator	Highest pressure	21.0
	Lowest pressure	19.0
	Pre-charge pressure	17.1
Low-pressure accumulator	Highest pressure	8.7
	Lowest pressure	6.2
	Pre-charge pressure	5.6

The simulation model described in Section 3 is used to simulate and analyze the robot movement. The input power and output power of each joint are shown in Fig.6.

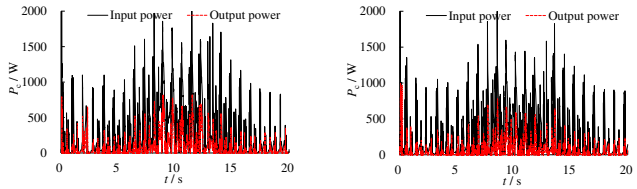

(a) Left Hip **(b) Right Hip**

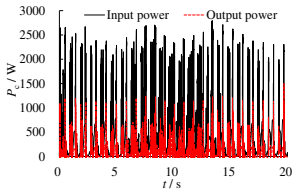

(c) Left Knee

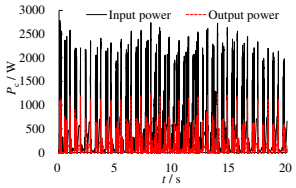

(d) Right Knee

Figure 6 Actuator input/output power after optimization

The input power of the hydraulic system after optimization is shown in Fig.7.

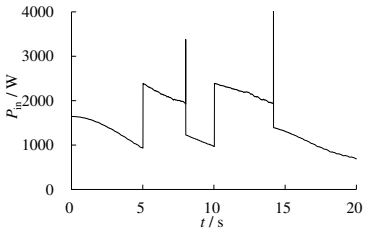

Figure 7 Input power of hydraulic system after optimization

After optimization, the active work and energy consumption of the hydraulic system is shown in Table 5.

Table 5 Active work and energy consumption after optimization

Component	Active work/J	Energy/J	Efficiency/%
Left hip cylinder	1910.27	5134.67	37.20
Right hip cylinder	1616.08	4662.51	34.66
Left knee cylinder	2538.17	9139.83	27.77
Right knee cylinder	2494.23	8850.20	28.18
Hydraulic system	8558.75	29650.77	28.87

5.2 Pressure without Optimization

In order to calculate the power and energy consumed by the hydraulic system and provide the comparison for the power unit pressure optimization algorithm, the power unit pressure without optimization control is obtained in this section.

Since the demand pressure of the hydraulic actuator is less than 10 MPa in most of the time, the pressure range of the low-pressure accumulator is set as 10~12MPa and the high-pressure accumulator is set as 19~21MPa. In this working condition, the input power and output power of each joint are shown in Fig.8, the input power of the hydraulic system is shown in Fig.9.

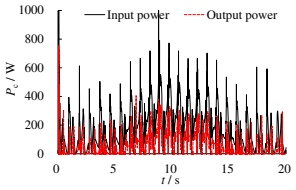

(a) Left Hip

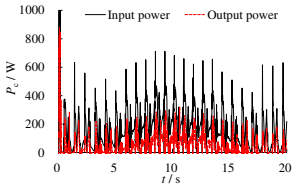

(b) Right Hip

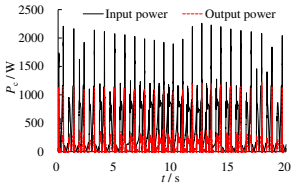

(c) Left Knee

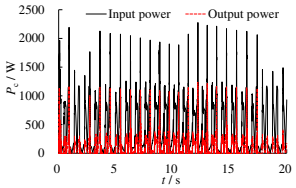

(d) Right Knee

Figure 8 Actuator input/output power without optimization

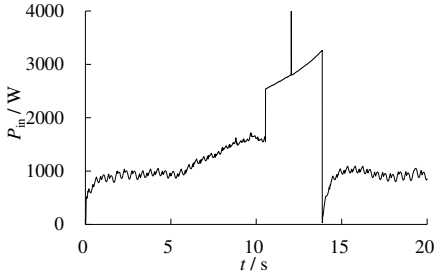

Figure 9 Input power of hydraulic system without optimization

Based on the calculation above, the active work and energy consumption of the hydraulic system can be obtained, as shown in Table .

Table 6 Active work and energy consumption without optimization

Component	Active work/J	Energy/J	efficiency/%
Left hip cylinder	1470.15	3672.94	40.03
Right hip cylinder	1325.02	3488.89	37.98
Left knee cylinder	2515.99	9764.15	25.77
Right knee cylinder	2411.53	9429.19	25.58
Power unit	7722.69	30425.88	25.38

5.3 Discussion

According to the simulation results, the overall efficiency of the hydraulic system optimized by the optimization algorithm is improved by 3.49%. The efficiency of the knee joint hydraulic cylinder increases by 2.00%~2.60, while the efficiency of the hip joint hydraulic cylinder decreases by

2.33%~3.32. Since the knee joint consumes more energy, the overall efficiency of the hydraulic system is improved.

During the switching process of high-pressure and low-pressure power source, it is easy to generate the impact force due to the sudden change of pressure. The impact force increases with the increase of pressure difference between high-pressure and low-pressure power source. The impact force will reduce the stability during movement. Also, the instantaneous flow into the actuator will increase at the impact moment, which will increase the instantaneous power and energy consumption of the joint actuator. According to the comparison between Fig.7 and Fig.9, the peak input power of hip actuator after optimization increases 45.31%~49.33%, and that of hip actuator increases 22.45%~23.56%. From the comparison between Table 5 and Table 6, after optimization, the active work of hip actuator increases 21.97%~29.94%, and the energy consumption increases 33.64%~39.80%; while the active work of knee actuator increases 0.89%~3.43%, but the energy consumption decreases 6.14%~6.39%.

According to the analysis of the above results, the power unit pressure optimization algorithm has a better energy saving effect on the knee actuator. The reason is that the output force of the knee joint actuator is smaller than that of the hip joint without considering the impact load due to the different joint torque. Therefore, appropriately reducing the low-pressure oil supply pressure of the power unit is conducive for the knee joint actuator to the full use of the low-pressure circuit. This will contribute to reducing the throttling loss and improving the efficiency of the knee joint actuator.

At the same time, the motion speed of the knee actuator is faster than that of the hip joint. The oil flow consumed by the knee actuator is more, which means that it will consume more energy. Therefore, reducing the energy consumption of the knee joint can reduce the overall energy consumption of the hydraulic system. As for the hip actuator, its working pressure is higher. So, the hip actuator will consume more oil from the high-pressure power source if the low-pressure power source supply pressure is reduced. If the pressure of the low-pressure power source is too low, the increased throttling loss of the hip actuator when using the high-pressure power source is greater than the energy saved by the decreased pressure of the low-pressure power source. So, the energy consumption of the hip actuator increases. To sum up, in order to further reduce the energy consumption of the hydraulic system, parameter matching of the hip and knee actuators should be carried out by combining the robot's geometric scale, locomotive gait and the force. Then, the pressure variation range will be closer to each other in the process of motion, so that the pressure from the power source can be utilized more effectively.

On the other hand, high speed on/off valve is adopted to improve the pressure switching speed of the actuator, which will contribute to improving the response speed and reducing the pressure loss during switching. However, the simulation results show that the switching process will produce large pressure fluctuations. The pressure fluctuations adversely affect stability and increase energy consumption. In order to analyze the influence of the high-pressure and low-pressure switching process on the system energy consumption, the simulation model is further modified in this paper. The two-position two-way proportional valve is used to realize the pressure switching. Integrating element and saturation element are added into the switching signal to make the pressure of the servo valve port P rise or fall along a slop signal. The switching time is set as 0.1s. In this model, the same movement gait is simulated and analyzed. The simulation results show that this method can reduce the impact force caused by pressure switching to a certain extent. But because of the delay of switching, the hydraulic system consumes more high-pressure power source to supply oil, which leads to the significant increase of energy consumption. Therefore, the selection of hydraulic system parameters needs to balance and optimize the contradiction between switching stability and energy consumption.

Finally, the fluid flow required by the hydraulic actuator during the walking process of the biped robot varies widely. For example, when both feet land on the ground, the hydraulic system requires a small flow rate due to the slow motion of the leg joints. As the leg moves forward, the hip and knee joints move faster. The hydraulic system consumes significantly more flow rate. With such flow characteristics, accumulator pressure also presents strong fluctuation. The response characteristics of hydraulic pump and electric motor make is hard for the pump output flowrate to accurately equal to the consumed flow rate all the time. The pump can only provide average flow rate. When the robot moves steadily with constant walking speed, the amount of oil consumed in each step is basically the same. The average flow of the hydraulic system is approximately a fixed value. In this case, the optimization algorithm can maintain the pressure variation range of the accumulator within the set value. The hydraulic system can make full use of the energy stored in the accumulator to achieve better energy saving effect. However, when the robot's walking speed changes, the average flow consumed by the actuator changes. The accumulator is prone to be under-charged, over-charged, or unable to reach the minimum set pressure, which makes the energy stored in the accumulator can not be fully used and the system energy consumption increases.

6 Conclusion

In this paper, an electric-hydraulic hybrid drive system is designed for the biped robot platform of Zhejiang Lab. The optimization algorithm of hydraulic power source pressure based on genetic algorithm is proposed. Firstly, the mathematical model of the hydraulic system is established. From the simulation analysis of the mechanical structure model, the motion characteristics and load characteristics of each joint under a specific action are obtained. Then, a value function reflecting the energy consumption of the hydraulic system is established. The value function calculates the energy consumption of the hydraulic system when a specific action is completed according to the pressure setting range of the low-pressure accumulator. A penalty function is introduced to control the switching time of the actuator between high and low pressure. Finally, genetic algorithm is used to calculate the low-pressure accumulator pressure setting range which makes the value function reaches the minimum value.

According to the simulation analysis, the efficiency of the optimized hydraulic system is 3.49% higher than that of the unoptimized one. However, since the pressure difference of the high-pressure and low-pressure power source is larger, it is easy to generate the impact force due to the sudden change of pressure. In order to further reduce the energy consumption of the hydraulic system, parameter matching of the hip and knee actuators should be carried out by combining the robot's geometric scale, locomotive gait and the force. Also, the selection of hydraulic system parameters needs to balance and optimize the contradiction between switching stability and energy consumption.

Availability of data and materials

The data that support the findings of this study are available from the corresponding author, [P.Y.Z.], upon reasonable request.

Conflict of interest statement

All authors disclosed no relevant relationships.

Funding

The work presented in this paper is supported by the Leading Innovation and Entrepreneurship Team of Zhejiang Province of China (Grant No. 2018R01006) and Ten Thousand Talents Program of Zhejiang Province (Grant No. 2019R51010).

Author contributions

P.Y.Z designed the study, performed the research, analysed data, and wrote the paper. The remaining authors contributed to refining the ideas, carrying out additional analyses and finalizing this paper.

Acknowledgements

The authors thank the Leading Innovation and Entrepreneurship Team of Zhejiang Province of China and Ten Thousand Talents Program of Zhejiang Province for

supporting this work.

References

[1] Biswal, P., & Mohanty, P. K. (2021). Development of quadruped walking robots: A review. Ain Shams Engineering Journal, 12(2), 2017-2031.

[2] Hu, K., Zhang, W., & Qi, B. (2021). Analysis and design of auto-adaptive leveling hydraulic suspension for agricultural robot. International Journal of Advanced Robotic Systems, 18(5), 17298814211040634.

[3] Yang, K., Zhou, L., Rong, X., & Li, Y. (2018). Onboard hydraulic system controller design for quadruped robot driven by gasoline engine. Mechatronics, 52, 36-48.

[4] https://www.maxonmotor.com.

[5] http://www.kollmorgen.com.

[6] Li, J., Cong, D., Yang, Y., & Yang, Z. (2021). A new bionic hydraulic actuator system for legged robots with impact buffering, impact energy absorption, impact energy storage, and force burst. Robotica, 1-18.

[7] Cho, B., Kim, M. S., Kim, S. W., Shin, S., Jeong, Y., Oh, J. H., & Park, H. W. (2021). Design of a Compact Embedded Hydraulic Power Unit for Bipedal Robots. IEEE Robotics and Automation Letters, 6(2), 3631-3638.

[8] Wang, X., Zhang, H., Zhang, X., & Quan, L. (2021, October). Design and Efficiency Analysis of Closed Loop Pump Controlled Circuit Hydraulic Lifting System of Wheel Loaders Based on Gravity Self-Balancing Hydraulic Cylinder. In Fluid Power Systems Technology (Vol. 85239, p. V001T01A038). American Society of Mechanical Engineers.

[9] Song, B., Lee, D., Park, S. Y., & Baek, Y. S. (2019). Design and performance of nonlinear control for an electro-hydraulic actuator considering a wearable robot. Processes, 7(6), 389.

[10] Shimizu, J., Otani, T., Mizukami, H., Hashimoto, K., & Takanishi, A. (2019, May). Experimental Validation of High-Efficiency Hydraulic Direct-Drive System for a Biped Humanoid Robot—Comparison with Valve-Based Control System. In 2019 International Conference on Robotics and Automation (ICRA) (pp. 9453-9458). IEEE.

[11] Ding, B., Plummer, A., & Iravani, P. (2019, July). Investigating balance control of a hopping bipedal robot. In Annual Conference Towards Autonomous Robotic Systems (pp. 171-182). Springer, Cham.

[12] Zhang, J., Yuan, Z., Dong, S., Sadiq, M. T., Zhang, F., & Li, J. (2020). Structural design and kinematics simulation of hydraulic biped robot. Applied Sciences, 10(18), 6377.

[13] Semini, C., Barasuol, V., Focchi, M., Boelens, C., Emara, M., Casella, S., ... & Caldwell, D. G. (2019). Brief introduction to the quadruped robot HyQReal. Istituto di Robotica e Macchine Intelligenti (I-RIM).

[14] Frigerio, M., Barasuol, V., Focchi, M., Caldwell, D. G., & Semini, C. (2018). Validation of computer simulations of the HyQ robot. In Human-Centric Robotics: Proceedings of CLAWAR 2017: 20th International Conference on Climbing and Walking Robots and the Support Technologies for Mobile Machines (pp. 415-422).

[15] Barasuol, V., Villarreal-Magaña, O. A., Sangiah, D., Frigerio, M., Baker, M., Morgan, R., ... & Semini, C. (2018). Highly-integrated hydraulic smart actuators and smart manifolds for high-bandwidth force control. Frontiers in Robotics and AI, 5, 51.

[16] Yang, K., Rong, X., Zhou, L., & Li, Y. (2019). Modeling and analysis on energy consumption of hydraulic quadruped robot for optimal trot motion control. Applied Sciences, 9(9), 1771.

[17] Sun, Y., Hua, Z., Li, Y., Hui, C., Li, X., & Su, B. (2021). Modeling and analysis on low energy consumption foot trajectory for hydraulic actuated quadruped robot. International Journal of Advanced Robotic Systems, 18(6), 17298814211062006.

[18] Ba, K., Song, Y., Yu, B., He, X., Huang, Z., Li, C., ... &

Kong, X. (2021). Dynamics compensation of impedance-based motion control for LHDS of legged robot. Robotics and Autonomous Systems, 139, 103704.

[19] Ba, K. X., Yu, B., Ma, G. L., Gao, Z. J., Zhu, Q. X., Jin, Z. G., & Kong, X. D. (2018). Dynamic Compliance Analysis for LHDS of Legged Robot, Part A: Position-Based Impedance Control. IEEE Access, 6, 64321-64332.

[20] Ba, K., Yu, B., Gao, Z., Zhu, Q., Ma, G., & Kong, X. (2018). Dynamic compliance analysis for lhds of legged robot, part b: Force-based impedance control. IEEE Access, 6, 74799-74811.

[21] Bao, R., Wang, T., & Wang, Q. (2019, July). A multi-pump multi-actuator hydraulic system with on-off valve matrix for energy saving. In 2019 IEEE/ASME International Conference on Advanced Intelligent Mechatronics (AIM) (pp. 1110-1115). IEEE.